African Journal of Environment and Natural Science Research
ISSN: 2689-9434
Volume 9, Issue 3, 2026 (pp. 113-128)
www.abjournals.org

SEISMIC ATTRIBUTE-BASED CHARACTERIZATION OF HETEROGENEOUS SAND RESERVOIRS IN THE NIGER DELTA BASIN, NIGERIA

Opiriyabo Ibim Horsfall[1], Onengiyeofori Anthony Davies[1*], Amonieah Jiriwari[1], and Mfonobong Joseph Akpan[2].

[1]Department of Physics, Rivers State University, Nkpolu - Oroworukwo P.M.B. 5080, Port Harcourt, Nigeria.

[2]Department of Physics (Geophysics Research Group), Akwa Ibom State University, Mkpat Enin, PMB 1162, Uyo, Nigeria.

[*]Corresponding Author's Email: davies.onengiyeofori@ust.edu.ng

Cite this article:

Opiriyabo, I. H., Onengiyeofori, A. D., Amonieah, J., Mfonobong, J. A. (2026), Seismic Attribute-Based Characterization of Heterogeneous Sand Reservoirs in the Niger Delta Basin, Nigeria. African Journal of Environment and Natural Science Research 9(3), 113-128. DOI: 10.52589/AJENSR-UL2U3OM4

Manuscript History

Received: 27 May 2026

Accepted: 29 Jun 2026

Published: 15 Jul 2026

Copyright © 2026 The Author(s). This is an Open Access article distributed under the terms of Creative Commons Attribution-NonCommercial-NoDerivatives 4.0 International (CC BY-NC-ND 4.0), which permits anyone to share, use, reproduce and redistribute in any medium, provided the original author and source are credited.

ABSTRACT: *Accurate characterization of heterogeneous reservoirs in the Niger Delta remains challenging because conventional seismic interpretation alone often fails to resolve complex structural features and lateral variations in reservoir properties. These limitations increase uncertainty in identifying hydrocarbon-bearing intervals and predicting reservoir continuity. This study integrates structural interpretation with seismic attribute analysis to improve reservoir characterization and hydrocarbon prospect identification in the onshore Omicron Field, Niger Delta, Nigeria. High-quality 3D seismic data, check-shot data, and well logs from four wells were integrated to delineate reservoir units, correlate lithologies, interpret faults and horizons, generate time and depth structure maps, and analyse coherency and root-mean-square (RMS) amplitude attributes. Two laterally continuous reservoir sands (Sand A and Sand B) were identified across the field, together with five major faults and two key seismic horizons. Structural interpretation revealed a fault-supported NW–SE-trending anticlinal closure, with structural highs concentrated in the central part of the field and structural lows toward the northwest. RMS amplitude maps show pronounced high-amplitude anomalies in the western part of both reservoirs, indicating potential hydrocarbon accumulation, while Sand B exhibits stronger amplitude responses than the shallower Sand A. The mapped fault-controlled closures and bright-spot anomalies collectively indicate favourable hydrocarbon potential within the study area. The results demonstrate that integrating seismic attributes with structural interpretation reduces uncertainty in reservoir characterization and provides a robust workflow for evaluating heterogeneous reservoirs and identifying exploration targets in the Niger Delta.*

KEYWORDS: Coherency; Faulting; Hydrocarbons; Reservoirs; RMS.

Article DOI: 10.52589/AJENSR-UL2U3OM4
DOI URL: https://doi.org/10.52589/AJENSR-UL2U3OM4

INTRODUCTION

As the demand for fossil fuels increases, reservoir characterization is becoming more and more important. By definition, reservoir characterization requires a thorough description of a reservoir using all the knowledge, methods, disciplines, and skills at hand. The output of reservoir characterization is a reservoir model that accounts for every aspect that affects a reservoir's ability to generate and store hydrocarbons. To identify structural and stratigraphic prospects and comprehend the rock and fluid properties within those prospects, the initial objective of any reservoir characterization inquiry is to give a high-quality image of the subsurface (Hossain et al. 2021). Reservoir geometry, including faults and facies variations that may have an impact on reservoir production performance, is taken into account during reservoir delineation. The physical characteristics of the reservoir, such as its porosity, permeability, water saturation, and pore fluid, are defined by the reservoir description.

A seismic attribute is any seismic data parameter that assists seismic interpreters in visually enhancing or quantifying characteristics of interpretation interest (Khayer et al., 2022). Seismic characteristics are a valuable tool for seismic interpretation. Seismic characteristics can be used to improve seismic data interpretation and are considered a powerful aid to seismic data interpretation. Seismic attributes are used to extract rock properties from observed seismic signals (Chopra & Marfurt, 2008; Torvela et al., 2013). They enable geoscientists to more quickly analyze faults and channels, determine the depositional environment, and unravel the structural deformation history. Seismic characteristics frequently aggregate subtle elements into groups by combining information from neighboring seismic samples and traces using a physical model (such as dip and azimuth, waveform similarity, or frequency content). A good seismic characteristic is either directly sensitive to the desired geologic feature or reservoir property of interest, or it allows us to describe the structural or depositional context and hence infer particular features or properties. One goal of seismic attributes is to quantify the amplitude and morphological traits perceived in seismic data using a system of deterministic calculations performed on a computer in order to capture the interpreter's pattern-recognition ability. For example, variance is a property that is used to identify or measure the coherence of the horizons; this also aids in the detection of faults because the area of low coherence indicates horizon fracture (Robinson & Davis, 2012; Ashraf et al., 2020).

Seismic structural interpretation aids in deciphering the architecture of subsurface strata by imaging minute features of geologic structures such as faults, folds, fracture networks, and so on (Mandal and Srivastava 2018). It gives light on the architecture of hydrocarbon-bearing beds as a result. When obtaining accurate images of these geologic features from geophysical data, interpreters frequently face significant obstacles. The application of structural geology ideas to seismic data interpretation is critical for correctly recreating subsurface structures and comprehending their geometric and kinematic evolution. This has a significant impact on prospect generation and exploration. The interpretation and identification of subsurface structural targets should always be supported by a complete understanding of the regional tectonic framework of the area, being aware of structural variability through space and time.

Due to the limitations of seismic resolution, accurate reservoir characterization has always been a tough undertaking. Dealing with diverse and heterogeneous reservoirs, which are common in the Niger Delta, makes this task all the more important. As a result, the main reasons for low hydrocarbon recovery efficiency are reservoir heterogeneities. Uncertainties regarding the lateral extent, distribution of reservoir properties (such as porosity, net pay thickness, fluid

Article DOI: 10.52589/AJENSR-UL2U3OM4
DOI URL: https://doi.org/10.52589/AJENSR-UL2U3OM4

type, and fluid saturation, etc.), and fault placements along the reservoirs are additional typical challenges in describing Niger Delta reservoirs (Inichinbia et al., 2014; Horsfall et al., 2017; Okeugo et al., 2018).

Because of the limitations of seismic resolution, reliable reservoir classification has always been difficult. Dealing with heterogeneous reservoirs, which are common in the Niger Delta, emphasizes the importance of this task. As a result, reservoir heterogeneities are the primary cause of low hydrocarbon recovery efficiency. Uncertainties about the lateral extent, distribution of reservoir properties (such as porosity, net pay thickness, fluid type, and fluid saturation, and so on), and fault placements along the reservoirs are also common challenges when describing Niger Delta reservoirs (Inichinbia et al., 2014; Horsfall et al., 2017; Okeugo et al., 2018). This study merges structural interpretation with seismic attribute analysis in an effort to address some of these challenges in order to anticipate and locate hydrocarbon-bearing reservoirs in a field, the onshore Niger Delta.

Geology and Location of the Study Area

The well logs and 3D seismic data used in this study were collected from *Omicron* oil field, which is located tens of kilometers Southeast of Port Harcourt in the Coastal Swamp Depositional Belt of the Niger Delta (Fig. 1). The field is located in Nigeria's Niger Delta sedimentary basin. The Niger Delta, which is located on the Gulf of Guinea and includes the Niger Delta provinces, is one of the world's most important hydrocarbon provinces (Klett et al., 1997). It is located between latitudes 4°N and 9°N and longitudes 4°E and 9°E. It is composed of a generally present regressive clastic succession with a maximum thickness of 12 km (Evamy et al. 1978). The Delta has prograded southward from the Eocene to the present, generating depobelts that characterize the Delta's most active region at each stage of its history (Doust & Omatsola 1990). With a surface area of around 300,000 km^2 (Kulke, 1995), a sediment volume of about 500,000 m^3 (Hospers, 1965), and a sediment thickness of more than 10 km in the basin depocenter (Kaplan et al., 1994), these depobelts constitute one of the largest regressive deltas in the world. According to Ekeweozor and Daukoru (1994), the tertiary Niger Delta (Akata - Agbada) petroleum system is the sole petroleum system found in the Niger Delta province.

Article DOI: 10.52589/AJENSR-UL2U3OM4
DOI URL: https://doi.org/10.52589/AJENSR-UL2U3OM4

ISSN: 2689-9434
Volume 9, Issue 3, 2026 (pp. 113-128)

Fig. 1 (a) Map of Africa and Nigeria in the inset (b) Map of the Niger Delta and its depositional belts indicating the location of the study area (after Adojoh et al. 2017) (c) Wellbore distribution across the study area

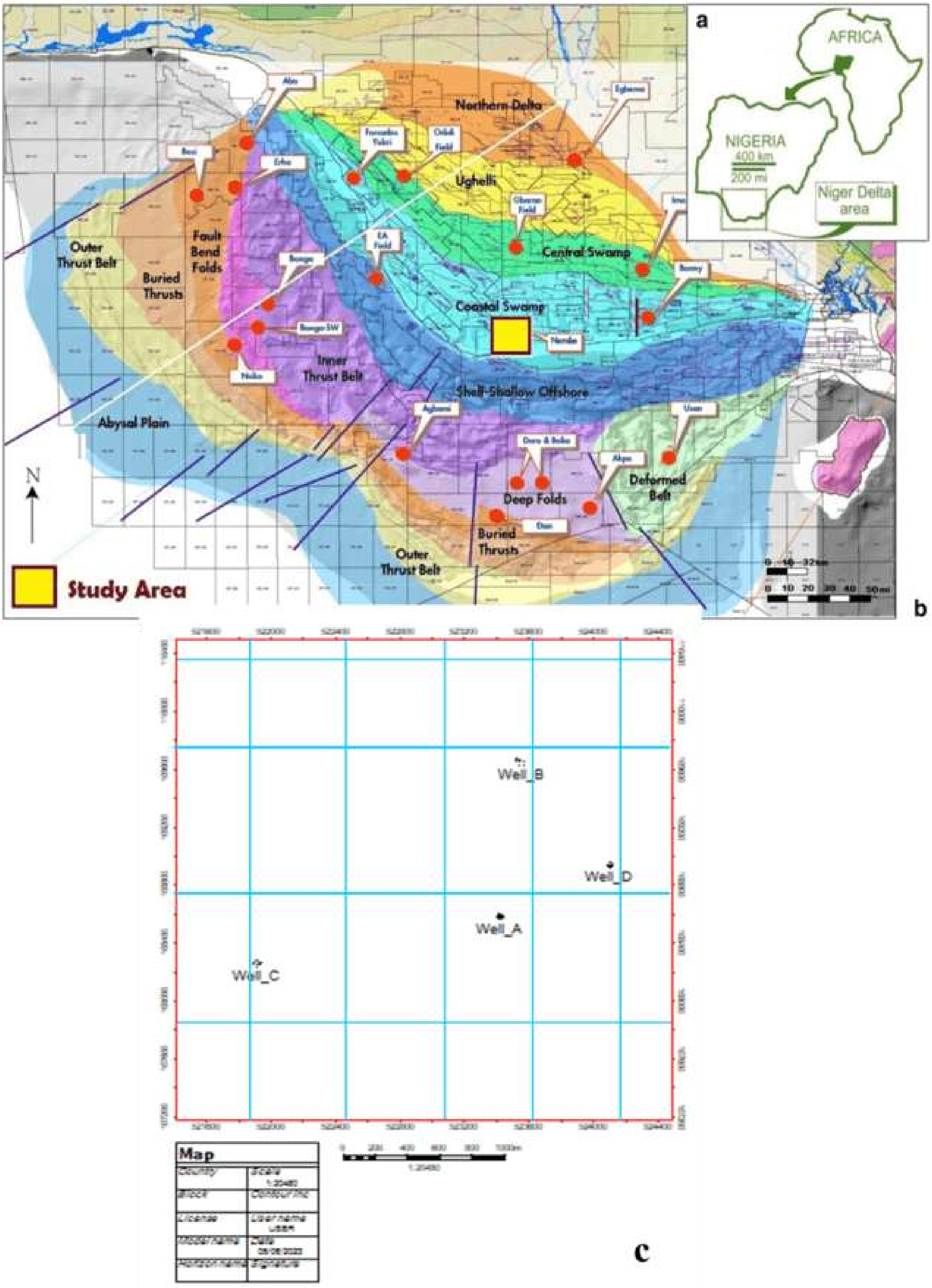

Article DOI: 10.52589/AJENSR-UL2U3OM4
DOI URL: https://doi.org/10.52589/AJENSR-UL2U3OM4

DATASETS AND METHODS

Datasets

The dataset used in this study, hereafter referred to as Omicron for confidentiality, is from the Coastal Swamp Depobelt of the Niger Delta Basin. It comprises a post-stack 3D seismic volume covering approximately 49 km² (7 km × 7 km), quality-controlled wireline logs from Wells A–D, well tops, checkshot surveys, rig-floor elevations, and ancillary well data. The available logs include gamma ray (GR, API), resistivity (RT, Ω·m), caliper (CAL, in), bulk density (RHOB, g/cm³), neutron porosity (NPHI, m³/m³), and sonic transit time (DT, µs/ft). The seismic volume consists of 496 inlines and 780 crosslines, yielding approximately 386,880 traces sampled at 4 ms. The data were provided as a processed post-stack migrated volume. Although the proprietary processing workflow, including migration, filtering, and amplitude-conditioning procedures, was unavailable, the dataset had undergone industry-standard quality control before release, including validation of the seismic and well-log data.

Identification of Reservoirs and Well Correlation

The first step in reservoir characterization research is often the delineation of reservoirs from logs. Gamma ray and resistivity records were used to identify probable hydrocarbon-bearing zones across the wells. For each of the wells, the sand baseline and the shale baseline were established. The shale baseline was chosen as having the highest mode GR occurrence, while the sand baseline was chosen as having the lowest mode GR occurrence at the lower spectrum. The middle point between the sand baseline and the shale baseline for each well was chosen as the sand/shale cut-off. Gamma ray values which deflect to the left of the established cut-off indicated clean sand while deflections to the right of the cut-off indicated shales. Well correlation was performed manually using gamma-ray and resistivity logs to establish lithostratigraphic continuity across the four wells. Correlation was based on the continuity of reservoir tops and bases, distinctive gamma-ray motifs, resistivity responses, and key marker shale horizons that served as regional correlation markers. Correlation lines were adjusted across mapped faults to account for fault-induced vertical displacement and preserve stratigraphic continuity. Correlation uncertainty was minimised through integration with seismic interpretation and well-top information, although local lithological variations and fault complexity may introduce minor ambiguities in reservoir continuity.

Fault Picking

Faults are observations of discontinuities or breaks in reflections in the hanging-wall and footwall cut-offs. The faults are mostly picked in the inline direction. The variance coherency property was utilized to aid in the depiction of faults that were difficult to identify in the original seismic data. Throughout the seismic data, both big and minor faults were identified. The faults were initially identified on the time slices using the variance property, then on the inline direction. This was required to calculate the horizontal extent of the fault traces (Odoh et al., 2014).

Horizon Mapping

The mapping of the principal horizons in the amplitude volume is an important step in seismic interpretation. Horizons reflection surfaces are visible in the data that have a similar wavelet structure throughout the survey. We can scan for potential fluid anomalies by mapping the

Article DOI: 10.52589/AJENSR-UL2U3OM4
DOI URL: https://doi.org/10.52589/AJENSR-UL2U3OM4

reflections and analyzing the amplitudes (Tschannen et al., 2020). Following the seismic-to-well tie process, horizon mapping began. The subsurface structure was interpreted seismically by selecting horizons along coherent reflections of the same phase. This usually translates to picks on a peak or trough in seismic surveys with zero phase correlation. These seismic responses (e.g., peaks and troughs) resemble differences in acoustic impedance between different earth materials. The faults picked were displayed on the seismic data, and the well tops were then toggled on.

Time Surface Generation

The seeded grids for the three horizons that were digitized were used as the input for generating the reservoir time structure surfaces. Before generating the surfaces, the fault traces on the seeded grids were mapped as polygons, which are ~~a~~ basic requirement for building a reservoir structural model (Zhang et al., 2022). The seeded grids were then converted to surfaces using a convergent interpolation algorithm. The surfaces were then contoured, and a seismic attribute called the surface attribute was applied to the surface to reveal the structural geometry. The digitized fault polygons were then eliminated from the time surfaces in order to reveal the exact positions and geometry of the fault traces as they truncate the surfaces.

Velocity Modelling

After the well seismic tie process was completed, the velocity function that gave the best match between the seismic and the synthetic seismic was preserved as the new Time Depth Relationship (TDR). The TDR function was utilized for converting the surfaces from time to depth. The TDR function was displayed graphically in a function window, and various polynomial functions were tested for a good fit (Ogbamikhumi & Aderibigbe, 2019). The third-order polynomial function gave the best fit to the velocity data and hence was used as the input for the velocity model conversion. The equation for the third-order polynomial function was utilized in the Petrel calculator for the conversion of surfaces from time to depth.

Depth Surface Generation

Depth surfaces were generated after the TDR function was run on the time surfaces. For a depth conversion to be considered good, the depth surfaces should show no significant differences in structure with the equivalent time structure surfaces. This goes a long way to say that the velocity function utilized for the depth conversion is very good. After depth conversion, the top structure maps that have been depth converted were used to generate the base structure map through an interpolation process called surface re-adjustment. The top surfaces were readjusted to generate the base surfaces using the well bases as input. The top and base structure maps were then used to determine the thickness of the reservoir surfaces using an isochore interpolation algorithm.

Seismic Attribute Analysis

A seismic attribute is a quantity extracted or derived from seismic data that can be analyzed to enhance information that might be subtler in a traditional seismic image, leading to a better geological or geophysical interpretation of the data (Kumar & Sain 2018). Coherency attribute and root-mean-square attribute were generated for this study. These attributes either reveal structure, lithology, or hydrocarbon presence. Coherency is a geometric seismic attribute that measures seismic continuity and is particularly useful in mapping the structure and shape of

Article DOI: 10.52589/AJENSR-UL2U3OM4
DOI URL: https://doi.org/10.52589/AJENSR-UL2U3OM4

geological features of interest, such as faults, anticlines, channels, and fractures. The Coherence discontinuity cube is essentially a cube of coherence coefficients generated from the input 3D seismic data volume, which portrays faults and other stratigraphic anomalies clearly, on time or horizon slices. RMS attribute is a post-stack attribute that computes the square root of the sum of squared amplitudes divided by the number of samples within the specified window used. With this root mean square amplitude, one can measure reflectivity to map direct hydrocarbon indicators in a zone of interest.

RESULTS AND DISCUSSIONS

Delineation of Hydrocarbon-Bearing Zones and Well Correlation

The first step in reservoir characterization research is often the delineation of reservoirs from logs. Using a combination of gamma ray and resistivity logs, two probable hydrocarbon-bearing zones were found across the wells. Table 1 shows the top, bottom, and gross reservoir thickness of the Sand A and Sand B reservoirs. The five wells were correlated across two (2) sand bodies known as Reservoir Sand A and Sand B. The wells have a typical Niger Delta formation of shale, sand, and shale sequence. Sand lithologies have high resistivities and minimal levels of gamma rays. The high gamma ray value aided in the classification of shale lithologies. Well correlation reveals the stratigraphy of the research field (Fig. 2). The correlation of lithostratigraphic intervals reveals that reservoir intervals are generally continuous laterally, with each sand unit running the length of the field, varying in thickness, and some units being deeper than their surrounding units. This is usually the outcome of faults present between the wells.

Table 1. A display of the top, bottom, and gross reservoir thickness of the Sand A and B reservoirs

Well Name	Reservoir Name	Reservoir Top Depth (Ft)	Reservoir Bottom Depth (Ft)	Gross Reservoir Thickness (Ft)
Well-A	SAND A	5823	6050	227
	SAND B	6090	6280	190
Well-B	SAND A	5730	6100	370
	SAND B	6085	6245	160
Well-C	SAND A	5860	6210	350
	SAND B	6210	6410	200
Well-D	SAND A	5820	5950	130
	SAND B	5970	6075	105

Article DOI: 10.52589/AJENSR-UL2U3OM4
DOI URL: https://doi.org/10.52589/AJENSR-UL2U3OM4

Fig. 2 Well section window showing the correlation across the five wells

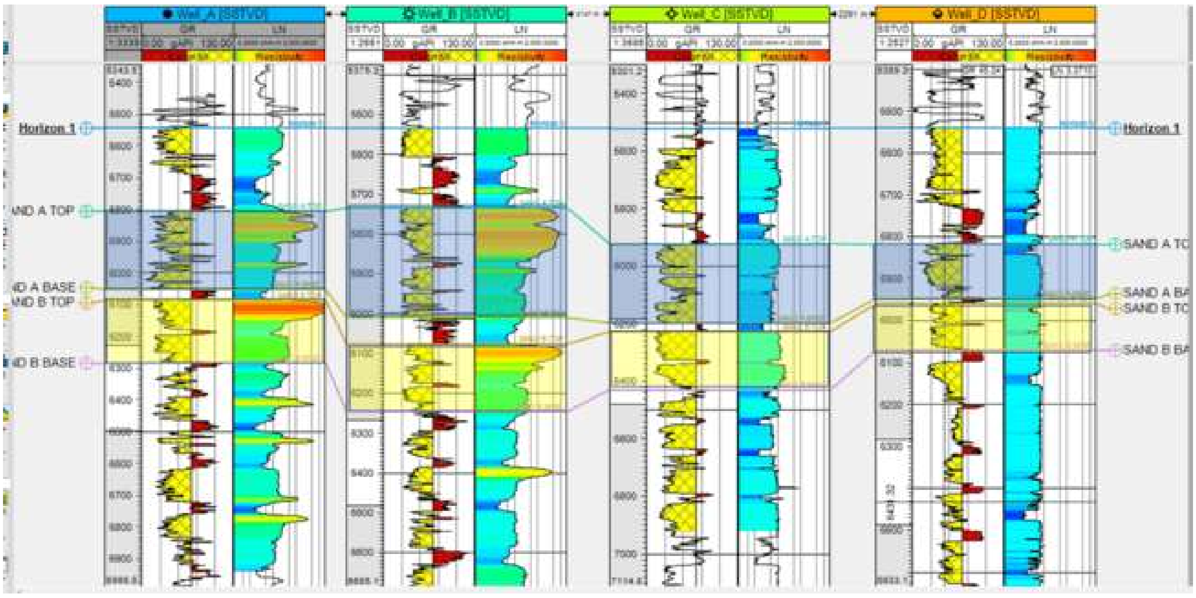

Fault and Horizon Interpretation

Fault and horizon interpretation were carried out to understand the structural architecture of the field. Fig. 3 shows variance coherency attributes (at 2000 seconds), which assisted in delineating major faults. Fig. 4 shows variance coherency attributes at 2000 seconds in 3D, highlighting subsurface geological discontinuities. Fig. 5 shows faults in a 3D view, showcasing fault geometries and spatial relationships. Fig. 6 shows an inline 5028 seismic section with horizons and formation tops for Sand A and B, respectively. Fig. 7 shows an inline 5028 seismic section displaying fault sticks and interpreted horizons. A total of 5 faults, labelled F1 to F5, were picked based on distortion of amplitude around a fault zone, sudden extinction of events, and variation in the dip of events. Fault 1 is considered a growth faults because it has thicker strata on the downthrown on the hanging wall side of the fault than in the footwall. The other faults labelled F2 to F5 are subsidiary faults. They are mostly listric and concave basin-wards. They are also synthetic, dipping in the same direction as the main fault. But fault 4, an antithetic fault, dips in the opposite direction. In most areas, interpreting fault plane geometry was difficult due to poor reflection characteristics around the fault, which is most likely a seismic acquisition and processing artifact (Marfurt & Alves, 2015; Alcalde et al., 2019; Akpan et al., 2020). Also, mapping fault detachments at depth is usually difficult, if not impossible, because data quality deteriorates significantly with depth due to energy attenuation (Bayowa et al. 2021).

Article DOI: 10.52589/AJENSR-UL2U3OM4
DOI URL: https://doi.org/10.52589/AJENSR-UL2U3OM4

African Journal of Environment and Natural Science Research
ISSN: 2689-9434
Volume 9, Issue 3, 2026 (pp. 113-128)

Fig. 3 A time slice through the variance coherency attributes (at 2000 seconds) to delineate faults

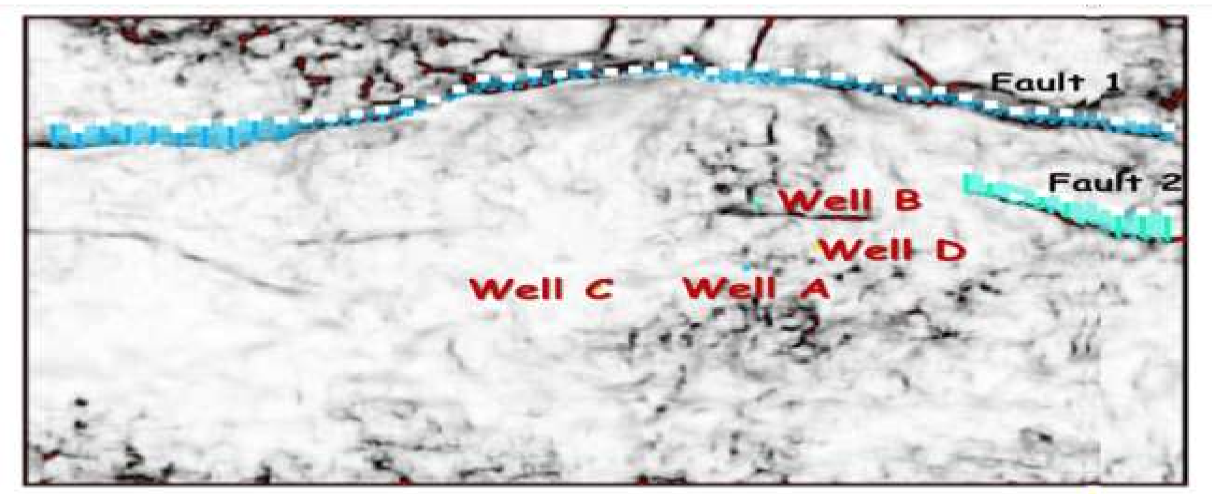

Fig. 4 Variance coherency attributes (at 2000 seconds) in 3D

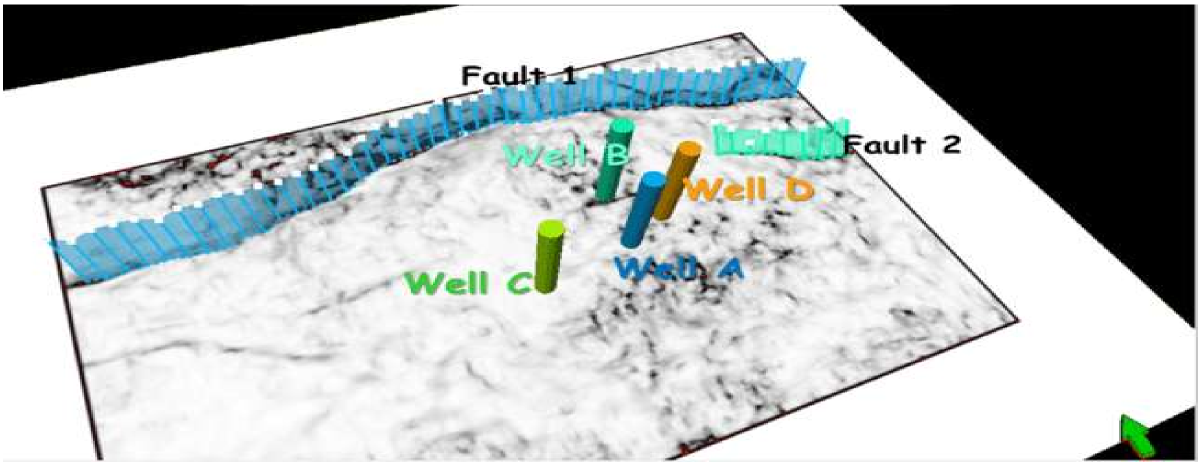

Fig. 5 Faults in 3D view

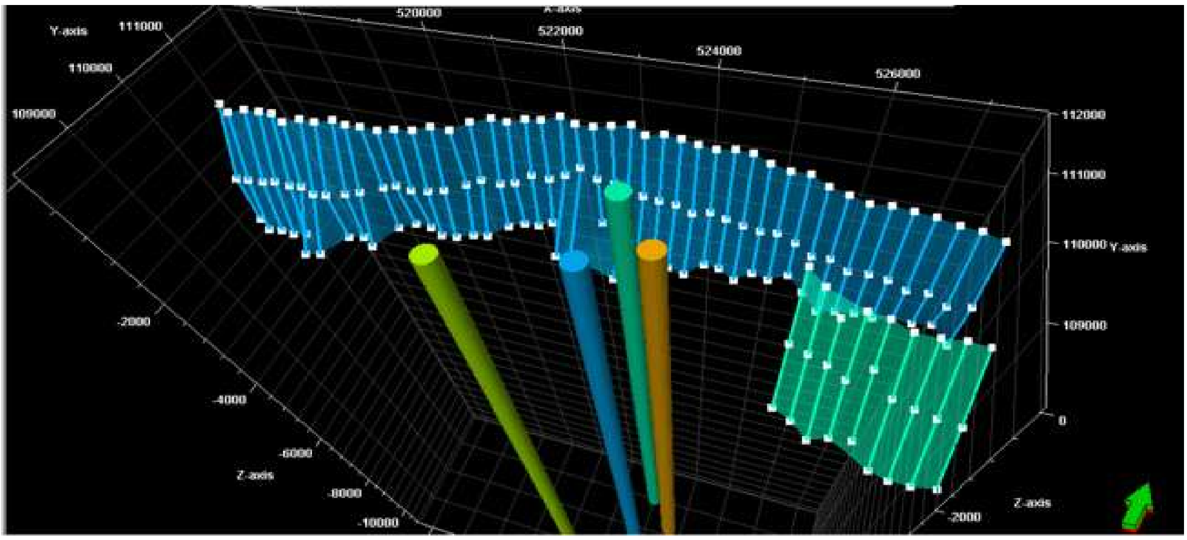

Article DOI: 10.52589/AJENSR-UL2U3OM4
DOI URL: https://doi.org/10.52589/AJENSR-UL2U3OM4

Fig. 6 Inline 5028 seismic showing Horizons and Formation tops for Sand A and B, respectively

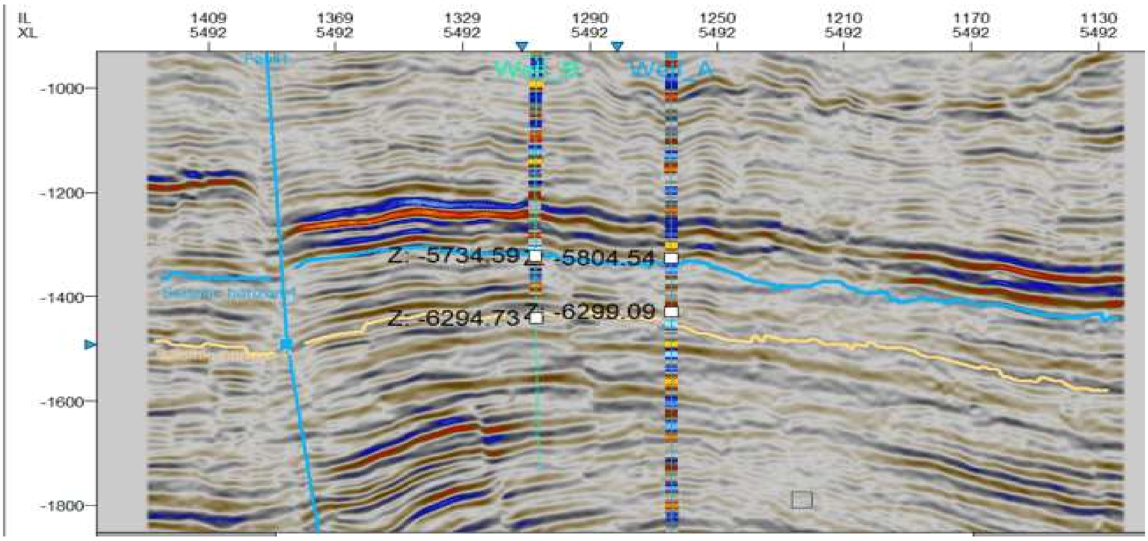

Fig. 7 Inline 5028 seismic showing fault sticks and interpreted horizons

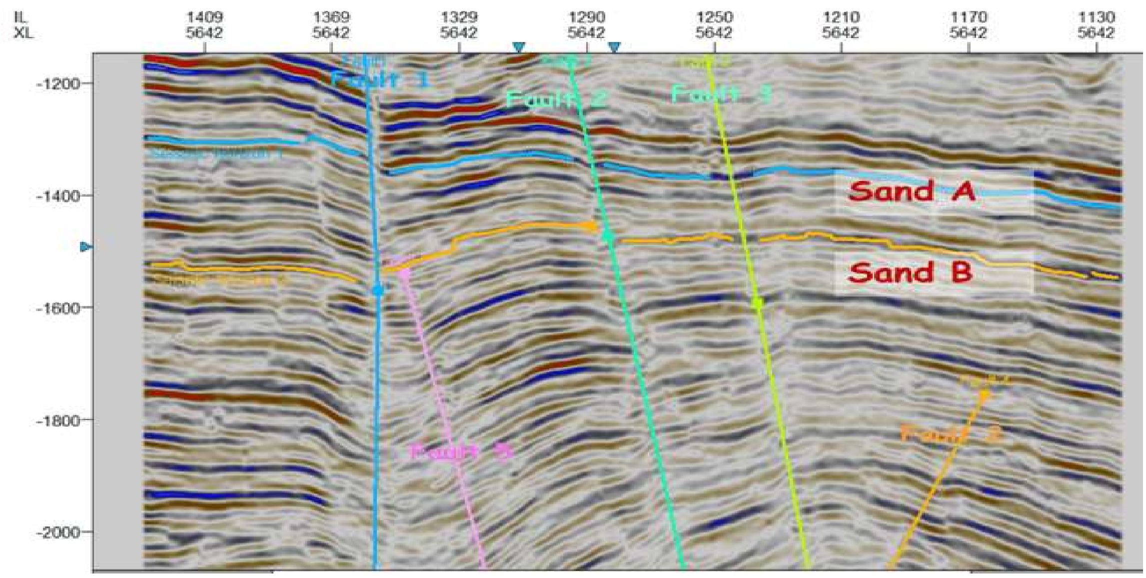

Time and Depth Structure Maps

Maps of time and depth structure were derived from the seismic volume. Fig. 8 depicts the reservoir time top structure map for Sand A, while Fig. 9 depicts the map for Sand B. Fig. 10 depicts the time-depth relationship curve. Fig. 11 shows a reservoir depth top structure map for Sand A with fault polygons, while Fig. 12 shows a map with fault polygons for Sand B. The wells were clustered along a NW-SE trending anticline, according to both time and depth structure maps. The horizons at 1295 ms (Sand A) and 1530 ms (Sand B) were differentiated by lateral reflection continuity with amplitudes of medium-high magnitudes. Furthermore, the inferred faults and seismic horizons revealed the field's structural texture and likely fault closures for hydrocarbon accumulation. The findings revealed that the survey region contains

Article DOI: 10.52589/AJENSR-UL2U3OM4
DOI URL: https://doi.org/10.52589/AJENSR-UL2U3OM4

African Journal of Environment and Natural Science Research
ISSN: 2689-9434
Volume 9, Issue 3, 2026 (pp. 113-128)

a number of fault-assisted closures, which could be places for hydrocarbon deposits. Using convergent interpolation, the temporal structural map was gridded to the interpreted horizon. Using the borehole and seismic data's time-depth connection, the time map was turned into a depth structural map (Fig. 10). The depth map depicts structure closures and other reservoir structural boundaries, such as faults. After time-to-depth conversion, the structural components on the time map were retained in the depth structural map. On the structural map, a NW-SE-trending anticlinal structure supported by faults can be seen in the northern portion of the area. In both reservoirs, structural highs are primarily found around the field's central region. Both reservoirs have similar structural lows in the field's northwest.

Fig. 8 Reservoir time top structure map for Sand A

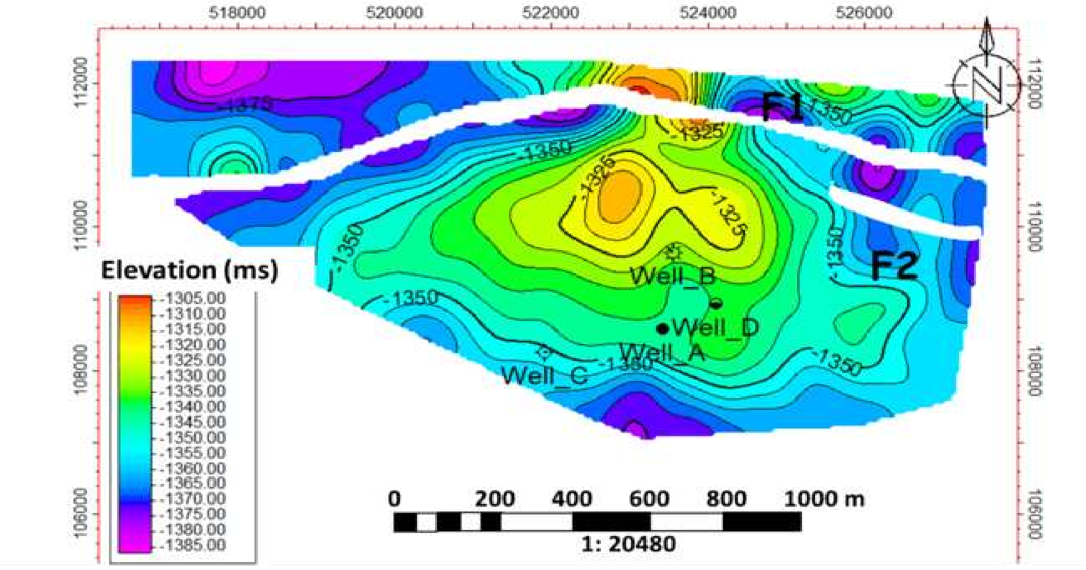

Fig. 9 Reservoir time top structure map for Sand B

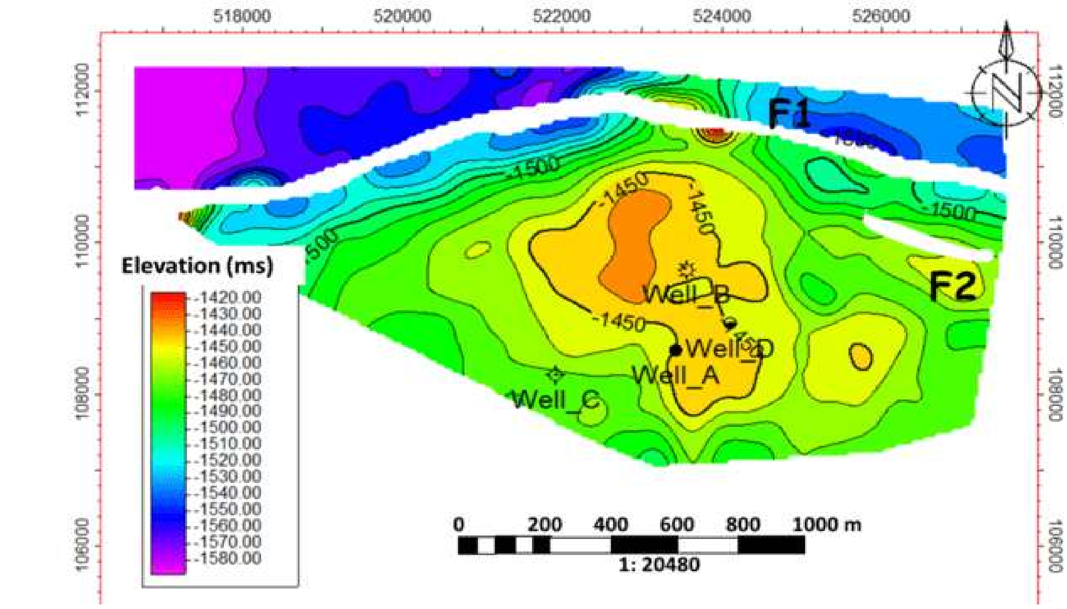

Article DOI: 10.52589/AJENSR-UL2U3OM4
DOI URL: https://doi.org/10.52589/AJENSR-UL2U3OM4

Fig. 10 Time-Depth Relation Curve

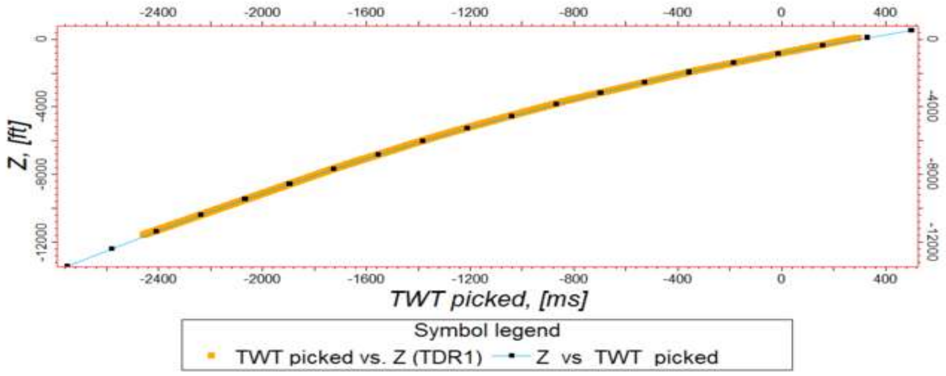

Fig. 11 Reservoir Depth top structure map showing fault polygons for Sand

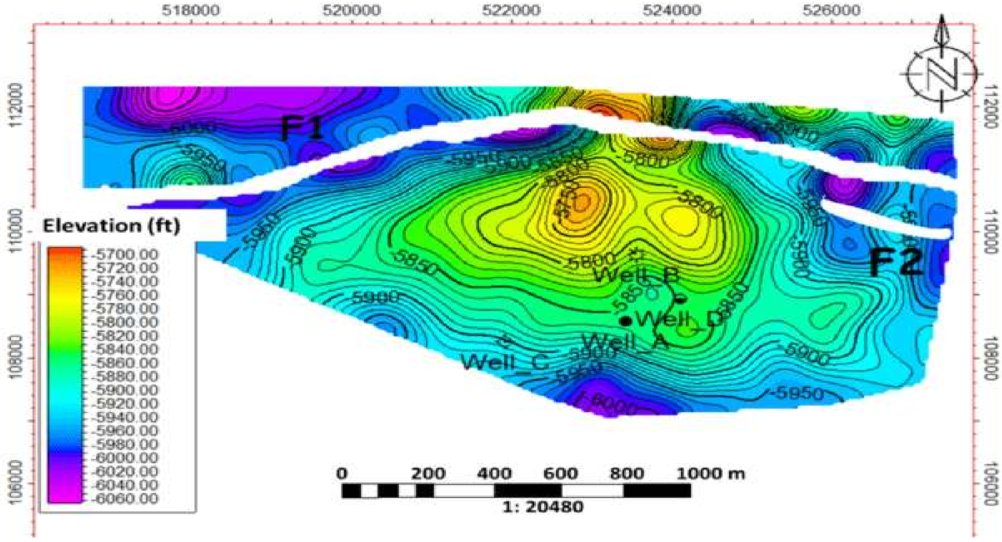

Fig. 12 Reservoir Depth top structure map showing fault polygons for Sand B

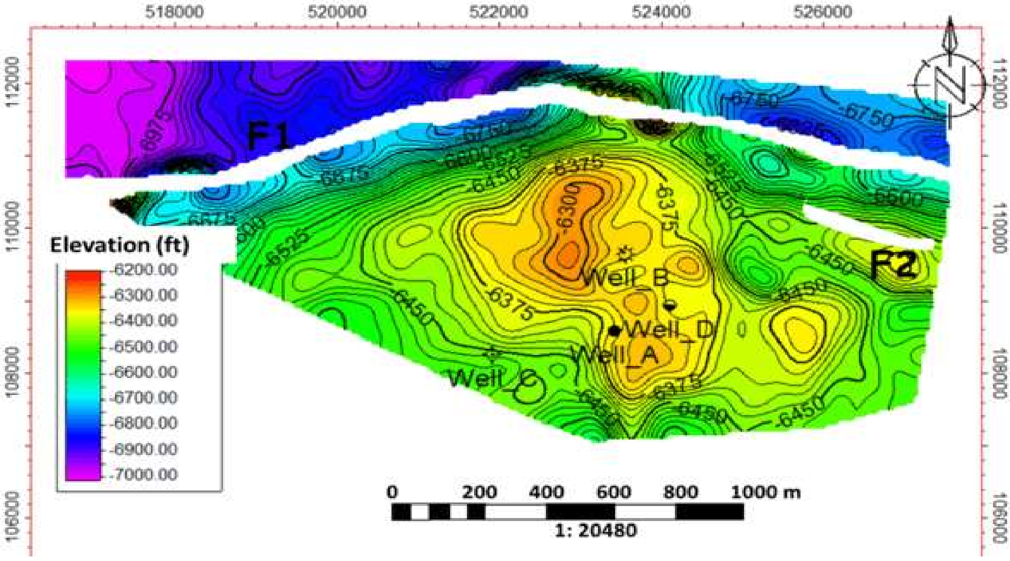

Article DOI: 10.52589/AJENSR-UL2U3OM4
DOI URL: https://doi.org/10.52589/AJENSR-UL2U3OM4

Seismic Attribute Analysis

Root mean square (RMS) amplitude and interval average arithmetic attribute maps were produced from the structural maps of both reservoirs, Sand A and Sand B. Fig. 13 and 14 show the RMS amplitude maps for the reservoirs Sand A and Sand B, while Fig. 15 and 16 depict the interval average arithmetic property for the reservoirs Sand A and Sand B, respectively. These characteristics were utilized to calculate reflectance in order to locate the most powerful direct hydrocarbon indication. The RMS and interval average arithmetic amplitude maps for the two horizons show the presence of both high and low amplitudes. The RMS amplitude maps show high amplitudes in and around the western sections of both reservoirs. This bright spot is generated by the presence of hydrocarbons. There are low amplitudes or dull areas around the well locations, indicating that the reservoir sands are likely very thin. Sand A has a higher concentration of low amplitudes than Sand B, which could be because Sand B occurs at a greater depth. The interval average arithmetic property follows a similar pattern, with low amplitude regions near well locations and high amplitude parts towards the western portions of the horizons. In general, the deeper sand B creates more amplitude than the shallower sand A.

Fig. 13 RMS Attribute Map of Sand A Reservoir

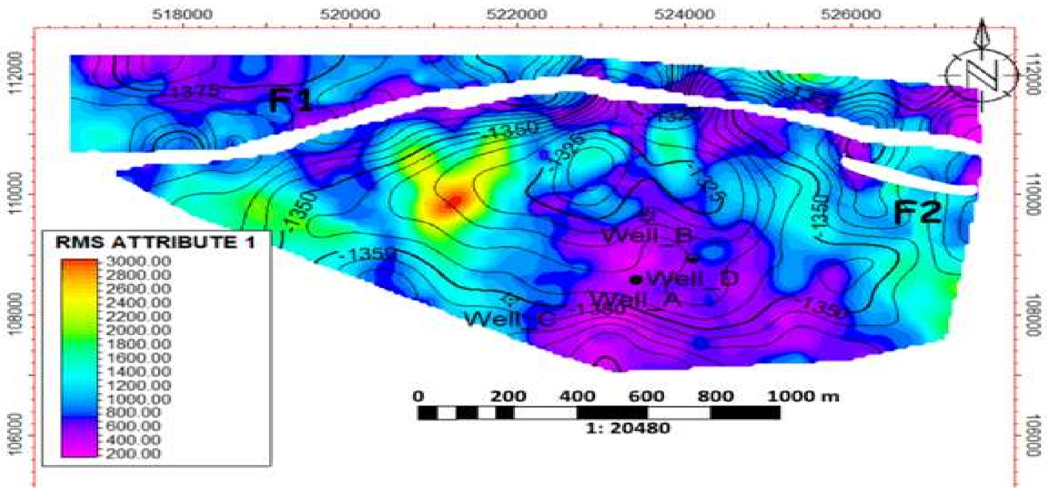

Fig. 14 RMS Attribute Map of Sand B Reservoir

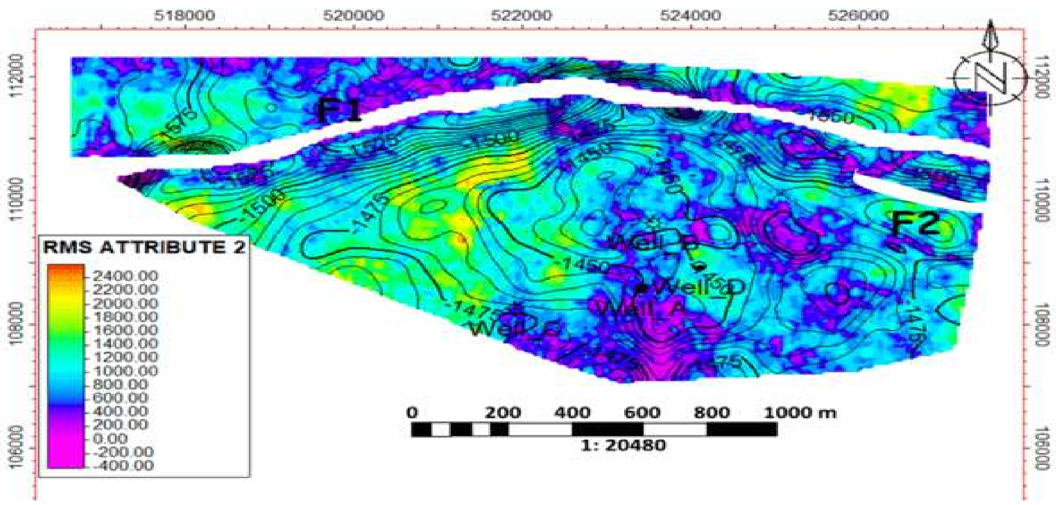

Article DOI: 10.52589/AJENSR-UL2U3OM4
DOI URL: https://doi.org/10.52589/AJENSR-UL2U3OM4

Fig. 15 Interval average arithmetic attribute extracted on Sand A

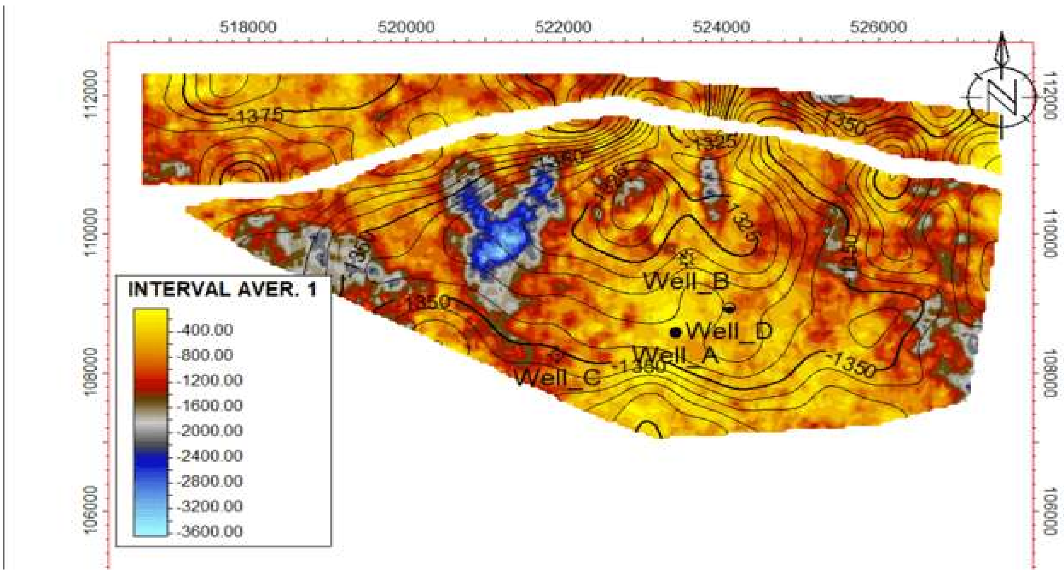

Fig. 16 Interval average arithmetic attribute extracted on Sand B

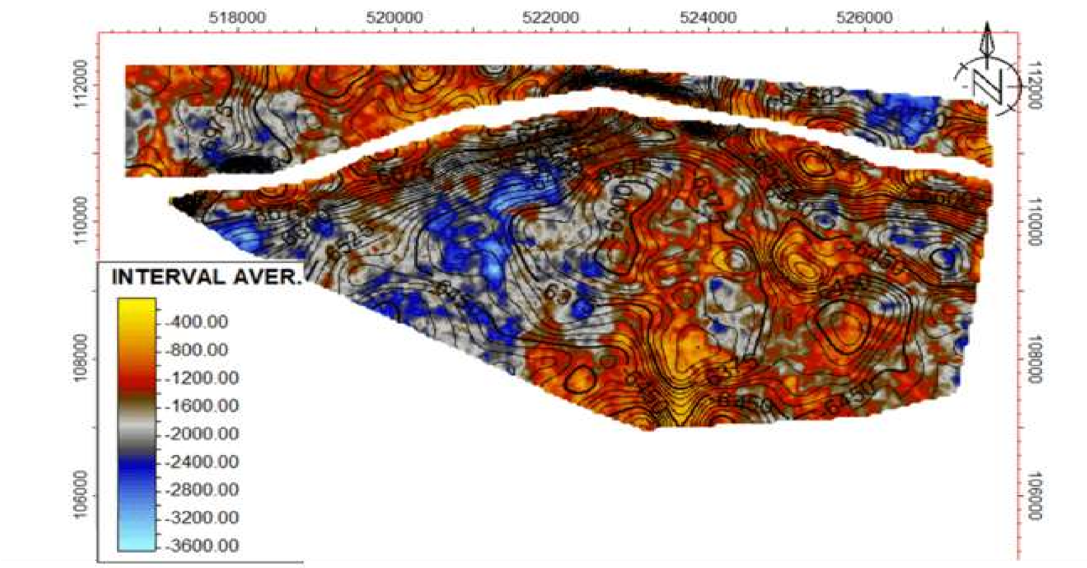

CONCLUSION

The findings of this study revealed the importance of 3D seismic features in reservoir assessment in the *Omicron* field, Coastal Swamp Depobelt, Niger Delta. Across the field, two separate reservoir sands from logs, five faults, and two horizons were mapped. According to the depth structure maps created, a NW-SE trending anticlinal structure was discovered in the research region. According to the RMS and interval average arithmetic amplitude maps, high amplitudes are present around the western parts of the two horizons. Because Sand B occurs at a deeper depth than Sand A, Sand A has a higher concentration of low amplitudes than Sand B. The bright spot, also known as strong reflections, indicates reservoir rocks with potential for hydrocarbon accumulation, as seen by seismic characteristics display maps. For a more

Article DOI: 10.52589/AJENSR-UL2U3OM4
DOI URL: https://doi.org/10.52589/AJENSR-UL2U3OM4

reliable characterisation of the *Omicron* field, seismic inversion, rock physics, and Amplitude Variation with Offset analysis should be conducted.

REFERENCES

Akpan, A. S., Okeke, F. N., Obiora, D. N., and George, N. J., 2020, Modelling and mapping hydrocarbon saturated sand reservoir using Poisson Impedance (PI) inversion: A case study of Bonna Field, Niger Delta Swamp Depobelt, Nigeria: Journal of Petroleum Exploration and Production Technology, Germany, 11, 117–132. https://doi.org/10.1007/s13202-020-01027-8.

Alcalde, J., Bond, C. E., Johnson, G., Kloppenburg, A., Ferrer, O., Bell, R., and Ayarza, P., 2019, Fault interpretation in seismic reflection data: An experiment analysing the impact of conceptual model anchoring and vertical exaggeration: Solid Earth, 10, 1651–1662. https://doi.org/10.5194/se-10-1651-2019.

Ashraf, U., Zhang, H., Anees, A., Ali, M., Zhang, X., and Shakeel Abbasi, S., 2020, Controls on reservoir heterogeneity of a shallow-marine reservoir in Sawan Gas Field, SE Pakistan: Implications for reservoir quality prediction using acoustic impedance inversion: Water, 12(11), 2972. https://doi.org/10.3390/w12112972.

Bayowa, O. G., Adagunodo, T. A., Oshonaiye, A. O., and Boluwade, B. S., 2021, Mapping of thin sandstone reservoirs in Bisol field, Niger Delta, Nigeria using spectral decomposition technique: Geodesy and Geodynamics, 12, 54–64. https://doi.org/10.1016/j.geog.2020.11.002.

Chopra, S., and Marfurt, K. J., 2008, Emerging and future trends in seismic attributes: The Leading Edge, 27(3), 298–318. https://doi.org/10.1190/1.2896620.

Doust, H., and Omatsola, E., 1990, Niger Delta: In Edwards, J. D. and Santogrossi, P.A., Eds., Divergent/passive margin basins: American Association of Petroleum Geologists Bulletin Memoir 48, 239–248.

Ekweozor, C. M., and Daukoru, E. M., 1994, Northern delta depobelt portion of the Akata-Agbada petroleum system, Niger Delta, Nigeria, in Magoon, L. B., and Dow, W. G., Eds. The Petroleum System--From Source to Trap, AAPG Memoir 60: American Association of Petroleum Geologists, 599-614.

Evamy, B. O., Herembourne, J., Kameline, P., Knap, W. A., Molloy, F. A., and Rowlands, P. H., 1978, Hydrocarbon habitat of Tertiary Niger Delta: American Association of Petroleum Geologists Bulletin, 62, 1-39.

Horsfall, O. I., Uko, E. D., Tamunoberetonari, I., and Omubo-Pepple, V. B., 2017, Rock-Physics and Seismic-Inversion Based Reservoir Characterization of AKOS Field, Coastal Swamp Depobelt, Niger Delta, Nigeria: IOSR Journal of Applied Geology and Geophysics (IOSR-JAGG), 5(4), 59–67. https://doi.org/10.9790/0837-0504035967.

Hospers, J., 1965, Gravity field and structure of the Niger Delta, Nigeria, West Africa: Geological Society of America Bulletin, 76, 407-422.

Hossain, M. S., Woobaidullah, A. S. M., and Rahman, M. J., 2021, Reservoir characterization and identification of new prospect in Srikail gas field using wireline and seismic data: Journal of Petroleum Exploration and Production Technology, 11, 2481–2495. https://doi.org/10.1007/s13202-021-01217-y.

Inichinbia, S., Sule, P., Ahmed, A. I., Hamza, H., and Lawal, K. M., 2014, Petrophysical analysis of among hydrocarbon field fluid and lithofacies using well log data: IOSR

Journal of Applied Geology and Geophysics, 2(2), 86–96. https://doi.org/10.9790/0990-02218696.

Kaplan, A., Lusser, C. U., and Norton, I. O., 1994, Tectonic map of the world, panel 10: Tulsa, American Association of Petroleum Geologists, scale 1:10,000,000.

Khayer, K., Roshandel-Kahoo, A., Soleimani-Monfared, M., and Kavoosi, K., 2022, Combination of seismic attributes using graph-based methods to identify the salt dome boundary: Journal of Petroleum Science and Engineering, 215, 110625. https://doi.org/10.1016/j.petrol.2022.110625.

Klett, T. R., Ahlbrandt, T. S., Schmoker, J. W., and Dolton, J. L., 1997, Ranking of the world's oil and gas provinces by known petroleum volumes: U.S. Geological Survey Open-file Report-97-463, CD-ROM.

Kulke, H., 1995, Nigeria, in Kulke, H., Ed., Regional Petroleum Geology of the World. Part II: Africa, America, Australia and Antarctica: Berlin, Gebrüder Borntraeger, 143-172.

Kumar, P. C., and Sain, K., 2018, Attribute amalgamation-aiding interpretation of faults from seismic data: An example from Waitara 3D prospect in Taranaki basin off New Zealand: Journal of Applied Geophysics, 159, 52-68. https://doi.org/10.1016/j.jappgeo.2018.07.023.

Mandal, A., and Srivastava, E., 2018, Enhanced structural interpretation from 3D seismic data using hybrid attributes: New insights into fault visualization and displacement in Cretaceous formations of the Scotian Basin, offshore Nova Scotia: Marine and Petroleum Geology, 89, 464–478. https://doi.org/10.1016/j.geog.2020.11.002.

Marfurt, K. J., and Alves, T. M., 2015, Pitfalls and limitations in seismic attribute interpretation of tectonic features: Interpretation, 3, SB5–SB15. https://doi.org/10.1190/INT-2014-0122.1.

Ogbamikhumi, A., and Aderibigbe, O. T., 2019, Velocity modelling and depth conversion uncertainty analysis of onshore reservoirs in the Niger Delta Basin: Journal of The Cameroon Academy of Sciences, 14(3). https://doi.org/10.4314/jcas.v14i3.7.

Okeugo, C. G., Onuoha, K. M., Ekwe, C. A., Anyiam, O. A., and Dim, C. I. P., 2019, Application of crossplot and prestack seismic-based impedance inversion for discrimination of lithofacies and fluid prediction in an old producing field, Eastern Niger Delta Basin: Journal of Petroleum Exploration and Production Technology, 9(1), 97–110. https://doi.org/10.1007/s13202-018-0508-6.

Robinson, H., and Davis, T., 2012, Seismic reservoir characterization of distributary channel sandstones in the Lower Cretaceous Paluxy reservoir, Delhi Field, Louisiana: In Proceedings SEG Technical Program Expanded Abstracts 2012 (Sutherland, Scotland: Society of Exploration Geophysicists), 1–6. https://doi.org/10.1190/segam2012-0164.1.

Torvela, T., Moreau, J., Butler, R. W. H., Korja, A., and Heikkinen, P., 2013, The mode of deformation in the orogenic mid-crust revealed by seismic attribute analysis: Geochemistry, Geophysics, Geosystems (G3), 14(4), 1069–1086. https://doi.org/10.1002/ggge.20050.

Tschannen, V., Delescluse, M., Ettrich, N., and Keuper, J., 2020, Extracting horizon surfaces from 3D seismic data using deep learning: Geophysics, 85, N17-N26. https://doi.org/10.1190/geo2019-0569.1.

Zhang, B., Tong, Y., Du, J., Hussain, S., Jiang, Z., Ali, S., Ali, I., Khan, M., and Khan, U., 2022, Three-dimensional structural modeling (3D SM) and joint geophysical characterization (JGC) of hydrocarbon reservoir: Minerals, 12(3), 363. https://doi.org/10.3390/min12030363.

Article DOI: 10.52589/AJENSR-UL2U3OM4
DOI URL: https://doi.org/10.52589/AJENSR-UL2U3OM4